A Wide-Range Trend Embrittlement Trend Curve for Western RPV Steels

Mark T Kirk†, mark.kirk@nrc.gov
Office of Nuclear Regulatory Research
US Nuclear Regulatory Commission, Washington, DC, USA

ABSTRACT

Embrittlement trend curves (ETCs) are used to estimate the magnitude of neutron irradiation embrittlement as a function of both exposure (fluence, flux, temperature, …) and composition (copper, nickel, manganese, phosphorus, silicon, …) variables. ETCs provide information needed to assess the structural integrity of operating nuclear reactors, and to determine their suitability for continued safe operation. As detailed by the table below, ETCs may use any of a number of different metrics to quantify the magnitude of embrittlement, and may use data from a number of different sources.

Embrittlement Metrics
Charpy *tanh* shift (ΔT_{41J})
Yield strength increase (ΔYS)
Hardness increase (ΔHv)
Fracture toughness transition shift (ΔT_o)

Data Sources	
Power Reactor Surveillance Irradiations	Country A
	Country B
	Country C
Test Reactor Irradiations	

Past efforts on ETC development in the United States have used data drawn from domestic licensees. For example, the ETCs in Regulatory Guide 1.99 Revision 2 and 10 CFR 50.61a were based on ΔT_{41J} data from Charpy specimens tested as part of licensee surveillance programs [RG199R2, 10CFR50.61a]. While this approach has addressed past needs well, future needs such as power uprates, license extensions to 60 years and beyond, and the use of low copper materials in new reactors produce future operating conditions for the US reactor fleet that may differ from past experience, suggesting that data from sources other than licensee surveillance programs may be needed. While data for these conditions is currently available, it is mostly quantified using embrittlement metrics other than ΔT_{41J}, and it arises mostly from sources other than the US surveillance program. In this paper we draw together embrittlement data expressed in terms of ΔT_{41J} and ΔYS from a wide variety of data sources as a first step in examining future embrittlement trends. Based on this evidence we develop a "wide range" ETC based on a collection of over 2500 data. We assess how well this ETC models the whole database, as well as significant data subsets. Comparisons presented herein indicate that a single algebraic model, denoted WR-C(5), represents reasonably well ***BOTH*** the trends evident in the data overall ***AS WELL AS*** trends exhibited by the following four data subsets:

- ΔT_{30} data from the US surveillance program
- ΔT_{30} data from non-US surveillance programs
- ΔT_{30} data from test reactor irradiations
- ΔYS data from test reactor irradiations

Of particular importance, the WR-C(5) model indicates the existence of trends in high fluence data (Φ > 2-3x10^{19} n/cm^2, E > 1MeV) that are not as apparent in the US surveillance data due to the limited quantity of ΔT_{30} data measured at high fluence in this dataset. Additionally, WR-C(5) models well the trends in both test and power reactor data despite the fact it has not term to account for flux. While the appropriateness of using data from such a variety of sources to inform a trend curve is debated by the technical community, it is suggested that one appropriate use of the WR-C(5) trend curve may include the design irradiation studies to validate or refute the findings presented herein. Additionally, WR-C(5) could be used, along with other information (e.g., other trend curves, theoretical expectations, plant-specific data, etc.), as one tool to predict irradiation trends pending the availability of confirmatory data in the high fluence régime.

† The views expressed herein are those of the author; they do not represent an official position of the United States Nuclear Regulatory Commission.

INTRODUCTION AND OBJECTIVE

Embrittlement trend curves (ETCs) are used to estimate the magnitude of neutron irradiation embrittlement as a function of both exposure (fluence, flux, temperature, …) and composition (copper, nickel, manganese, phosphorus, silicon, …) variables. ETCs provide information needed to assess the structural integrity of operating nuclear reactors, and to determine their suitability for continued safe operation. As detailed by the table below, ETCs may use any of a number of different metrics to quantify the magnitude of embrittlement, and may use data from a number of different sources.

Embrittlement Metrics	Data Sources	
Charpy *tanh* shift (ΔT_{41J})	Power Reactor Surveillance Irradiations	Country A
Yield strength increase (ΔYS)		Country B
Hardness increase (ΔHv)		Country C
Fracture toughness transition shift (ΔT_o)	Test Reactor Irradiations	

Past efforts on ETC development in the United States have used data drawn from domestic licensees. For example, the ETCs in Regulatory Guide 1.99 Revision 2 and 10 CFR 50.61a were based on ΔT_{41J} data from Charpy specimens tested as part of licensee surveillance programs [RG199R2, 10CFR50.61a]. While this approach has addressed past needs well, future needs such as power uprates, license extensions to 60 years and beyond, and the use of low copper materials in new reactors produce future operating conditions for the US reactor fleet that may differ from past experience, suggesting that data from sources other than licensee surveillance programs may be needed. While data for these conditions is currently available, it is mostly quantified using embrittlement metrics other than ΔT_{41J}, and it arises mostly from sources other than the US surveillance program. In this paper we draw together embrittlement data expressed in terms of ΔT_{41J} and ΔYS from a wide variety of data sources as a first step in examining future embrittlement trends. Based on this evidence we develop a "wide range" ETC based on a collection of over 2500 data.

ANALYTICAL APPROACH

We have adopted an empirical analysis approach, collecting published data to obtain the information needed to inform an ETC. Past ETCs developed by the NRC have been calibrated using only ΔT_{30} data obtained from the USLWR surveillance program [Randall 87, Eason 98, Eason 07]. This previous approach excludes data from test reactor irradiations, it excludes data from non-US surveillance programs, and it excludes studies that used metrics other than ΔT_{30} to quantify embrittlement. Unfortunately, it is mostly from these excluded data sources where one finds most of the data that is now available to characterize the high fluence levels that will occur during extended operations, as well extensive data on the low copper materials that are expected to be used for the construction of new reactors. For example:

- Test reactor data is predominant in the high fluence regime because such data can be generated in limited periods of time because of the high fluxes that can be achieved in test reactors. While many test reactor studies use ΔT_{41J} as the embrittlement metric, two recent and quite extensive studies have instead used ΔYS.
- High fluence data is more commonly found in non-US surveillance than it is in US surveillance. This limitation to the US surveillance program occurs because the current provisions of the NRC's Generic Aging Lessons Learned, or GALL, report require that licensees remove their capsules when they have accumulated a fluence equivalent to 60 years operating at full power [GALL]. This limitation makes it nearly impossible for licensees to generate high fluence data while remaining compliant with the GALL recommendations.

In addition to these pragmatic reasons to include data from non-traditional sources, another motivation to use such data arises from the observation that *a priori* exclusion of data that may be relevant to the prediction of future conditions in commercial power reactors is not good practice because it eliminates such data from consideration without an assessment of its relevance. Conversely, admission of such data to the analysis allows quantitative assessment of if the data should have been included, or if there are technical reasons to justify its exclusion. In all cases, the appropriateness of use data from non-traditional sources (i.e., test reactors, non-US surveillance, and ΔYS data) is assessed by comparing trends exhibited by the different data sources.

EMPIRICAL DATABASE

The empirical database that forms the basis for the fits presented in this paper was assembled from the technical literature. As detailed in Table 1, this database contains both power and test reactor data where the magnitude of

neutron irradiation embrittlement has been quantified using one of two metrics: ΔT_{30} or ΔYS. In cases where ΔYS values were reported they were converted to ΔT_{30} values using the following relationship, which is based on RPV steel data for which both ΔYS and ΔT_{30} data are available [Kirk 01]:

$$\Delta T = \gamma \cdot \Delta YS \quad (1)$$

In eq. (1) if ΔT is expressed in °C and ΔYS is expressed in MPa, then γ = 0.69, 0.60, and 0.49 °C/MPa for welds, plates, and forgings respectively. Conversely, if ΔT is expressed in °F and ΔYS is expressed in ksi, then γ = 8.56, 7.45, and 6.08 °F/ksi for welds, plates, and forgings respectively.

Slightly over a third of the database (37%) comes from US power reactor data; this is augmented by another 11% of the database from overseas power reactors, with the remainder of the data (52%) coming from test reactors. Roughly three of every five test reactor shift values are a measurement of ΔYS rather than ΔT_{30}. Only a very small portion of the power reactor data has embrittlement quantified using ΔYS. An examination of the various data sets makes clear that the USLWR power reactor data occupies a similar composition range to data from other sources. Conversely, Figure 1 shows that while US and non-US power reactor data occupy similar ranges of exposure variables, these data exhibit the known and expected differences between the exposures experienced test and power reactors, and indeed between the two power reactor types: pressurized water reactors (PWRs) and boiling water reactors (BWRs).

Table 1. Summary of Empirical Database.

Citation	Reactor Type		Embrittlement Metric		# of Datum	Description
	Power	Test	ΔT_{30}	ΔYS		
Eason 07	X		X		936	US power reactor surveillance database through 2002
Eason 07		X		X	390	IVAR test reactor data on RPV alloys only (model alloy data are also available, but were not used in fitting)
Chaouadi 05a		X		X	358	Test reactor data on western RPV alloys (VVER data also available, but not used in fitting)
Stallmann 94	Few	mostly	X		263	Database on pre-1990 test reactor data
IAEA CRP-1, 2, 3		X	X		142	Test reactor data on western RPV steels developed as part of International Atomic Energy Agency (IAEA) Cooperative Research Projects 1, 2, and 3.
Brillaud 92	X		X		122	French power reactor surveillance database through 1992 (predominantly data on low Cu forging alloys)
JNES 07	X	X	X		99	Data from Japan on western RPV steels under both power and test reactor conditions
Bellman 90		X	X		65	Data on several western RPV steels
Fabry 96	X	X	X		59	Data on Yankee Rowe welds and plates
Gérard 06	X	X		X	56	Data on low copper forgings and welds exposed under both power and test reactor conditions
Brillaud 01	X		X		17	Trepan data from the Chooz-A vessel (France)
Hawthorne 85	X	X	X		11	
Ishino 90		X	X		11	
Kussmaul 90	X		X		8	Trepan data from the Gundremmingen vessel (Germany)
Onizawa 01		X	X		8	Data on several western RPV steels
Pachur 93		X	X		5	
Leitz 93		X	X		5	
Nanstad 04		X	X		4	Data on the correlation monitor material JRQ
Lee 01		X	X		2	

FITTING PROCEDURE

Fitting Form

The functions used to fit the data were motivated more by pragmatic concerns associated with developing good representations to empirical trends than by concerns associated with making fitting functions conform to insights from current and, in many cases, still developing theoretical constructs. This does not imply an approach deaf to theoretical insights, but rather suggests an emphasis on identifying clear trends in the data and adopting functions that follow these trends. The fit to the database begins with observation of the following strong data trends, which are illustrated in Figure 3:

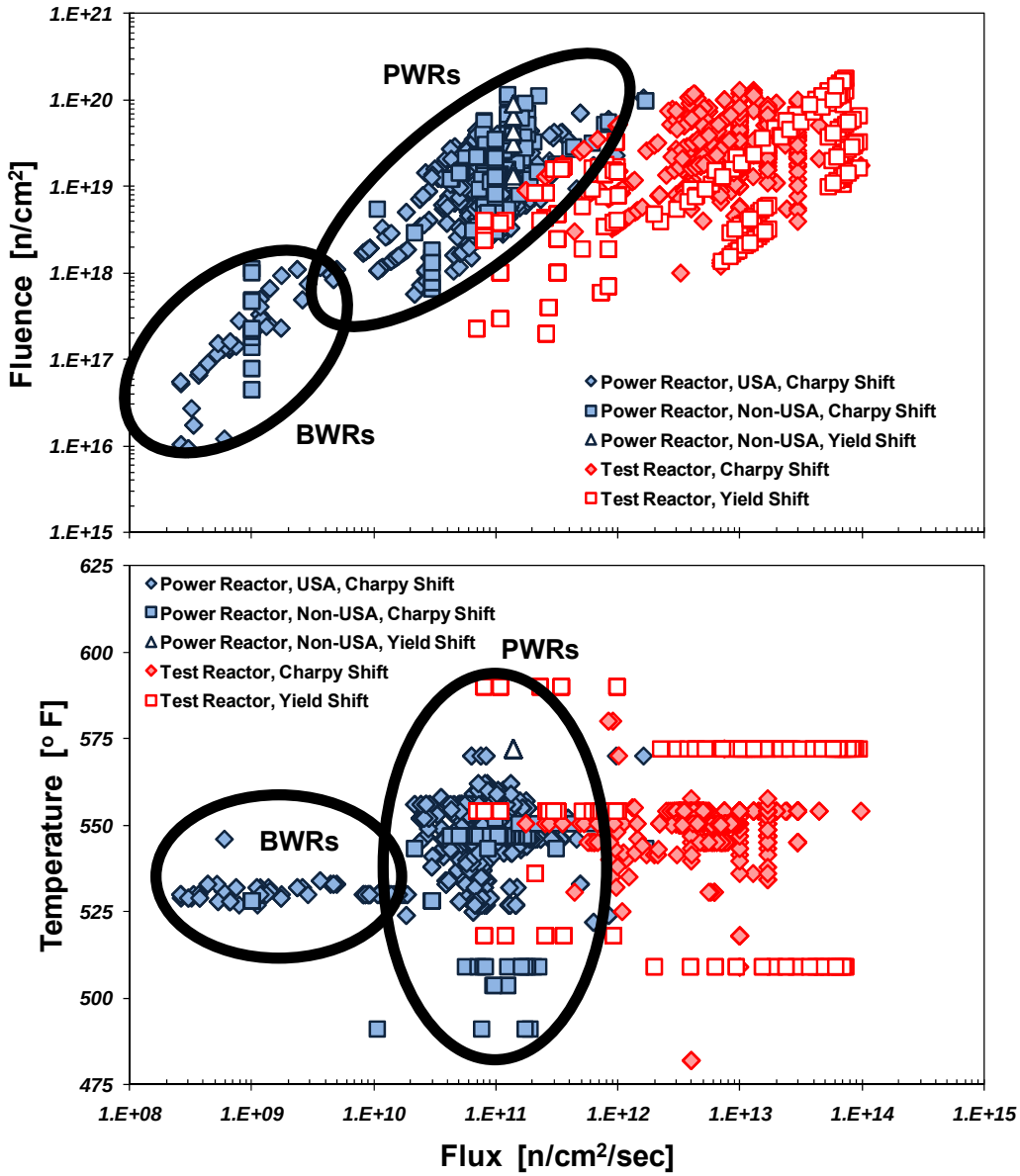

Figure 1. Exposure ranges in database (Power reactor data in blue, test reactor data in red).

- Between a minimum value of copper (Cu_{MIN}) and above a maximum value of copper (Cu_{MAX}) the slope on a plot of ΔT_{30} *vs*. Cu increases with increasing fluence up to a saturation fluence of about 1.5×10^{19} n/cm^2. As fluence increases above about 1.5×10^{19} n/cm^2 this slope remains constant.
- Below Cu_{MIN} and above Cu_{MAX} there is no dependence of ΔT_{30} on copper content.
- The value ΔT_{30} below Cu_{MIN} increases without any apparent bound as fluence increases.

The plots in Figure 3 adopt values of Cu_{MIN} = 0.07 and Cu_{MAX} = 0.30. These values were established by observing similar plots having Cu_{MIN} ranging from 0.05 to 0.10 and Cu_{MAX} ranging from 0.25 and 0.35. The values of 0.07 and 0.30 were selected to best partition the Cu-sensitive and Cu-insensitive data regions. It may be noted that these Cu_{MIN} and Cu_{MAX} values are in reasonable accord with those adopted by other investigators [Chaouadi 05a, Chaouadi 05b, IAEA 1442, Williams 86].

shows the variations of M_Φ (the slope on Figure 3 between Cu_{MIN} and Cu_{MAX}) and B_Φ (the average value of ΔT30 below Cu_{MIN}) with fluence established by least-squares fitting of plots such as those in Figure 3. These variations provide the starting point for an ETC model of the general form:

$$\Delta T_{30} = MAX\left\{\frac{MIN(Cu, Cu_{MAX}) - Cu_{MIN}}{0}\right\} \times M + B \qquad (2)$$

where

Cu_{MIN} =	0.07 wt-%	Cu_{MAX} =	0.30 wt-%

The result of eq. (2) is expressed in °F; multiplication by $\frac{5}{9}$ provides a result in °C. In eq. (2) the "M" and "B" terms are modifications of M_Φ and B_Φ to account for the effect of composition variables, exposure variables, and categorical variables that have not been controlled in the plots in Figure 3. The form of the "M" and "B" terms are as follows:

$$M = MIN\{[ln(\Phi) - ln(\Phi_{TH})] \cdot M_\Phi, M_{\Phi-max}\} \cdot [Modification\ Terms] \qquad (3)$$

$$M_{\Phi-max} = M_\Phi \cdot [ln(\Phi_{Cu-SAT}) - ln(\Phi_{TH})] \qquad (4)$$

$$B = \{C \cdot \Phi^D\} \cdot [Modification\ Terms] \qquad (5)$$

where

Cu_{MIN} =	0.07 wt-%	Cu_{MAX} =	0.30 wt-%
M_Φ =	158.28 °F/wt%	$M_{\Phi\text{-max}}$ =	728.9 °F/wt%
Φ_{TH} =	$1.5\text{x}10^{17}$ n/cm^2	$\Phi_{Cu\text{-SAT}}$ =	$1.5\text{x}10^{19}$ n/cm^2
C =	$1\text{x}10^{-9}$	D =	0.5502

The model described by Eqs. (2-5), with modification terms set to unity, represents the database reasonably well for such a simple model, but there are significant residual trends with respect to many variables and the model has a high standard error (48.5 °F) relative to other models reported in the literature. These observations suggest the need for modification terms to obtain a model that provides a more thorough representation of the trends exhibited by the data.

To reduce to statistical insignificance any un-modeled residual trends the following general form was adopted for a modification term:

$$MOD_X = \left[\frac{X^P}{X_{MEAN}}\right]^E \qquad (6)$$

In eq. (6) the term MOD_X is interpreted as the "modification for variable X" where "X" may be either a composition variable (Ni, Mn, P, Si) or an exposure variable (fluence, temperature). In the fitting process "MOD_X" terms are added to both eq. (3) and eq. (5) as needed to reduce to statistical insignificance the
the residual trends. The value "X" in the numerator is the value of that variable for the ΔT_{30} observation of interest, while the value X_{MEAN} in the denominator is the mean value of that variable for the entire ETC database. The values of "P" and "E" are established by the least-squares fitting process to best represent the trends in the database. Figure 4 illustrates the values of MOD_X produced by eq. (6) for various combinations of "P" and "E," demonstrating that eq. (6) is a very adaptable function that is capable of providing both linear and non-linear modifications, as dictated by the trends in the ETC database.

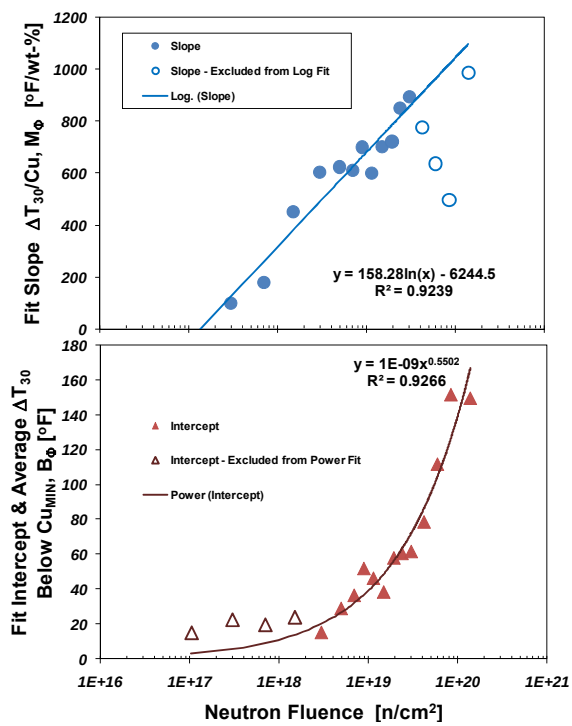

Figure 2. Variations of M_Φ and B_Φ with fluence established by least-squares fitting of plots such as those in Figure 3.

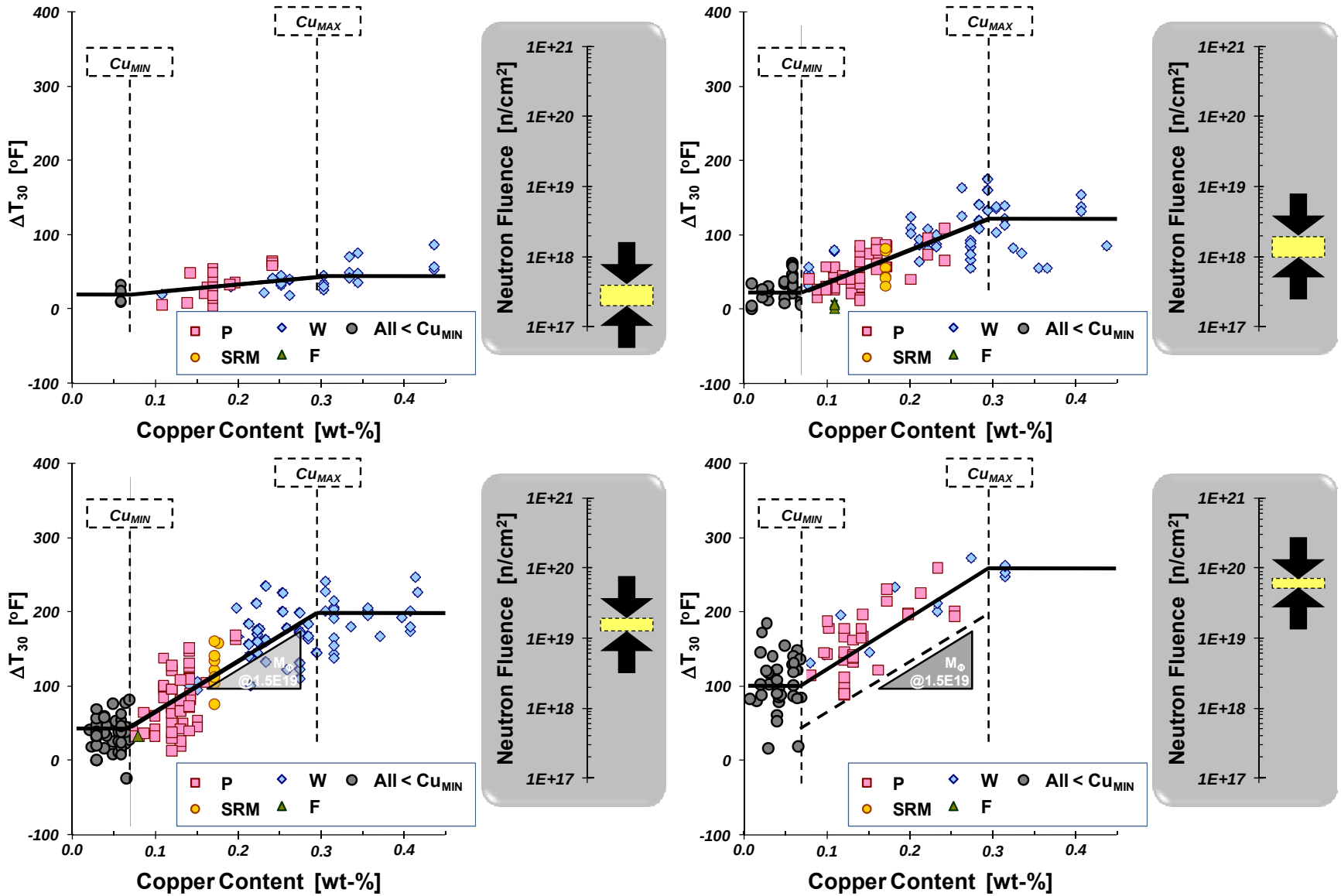

Figure 3. Embrittlement shift data displayed over limited fluence ranges.

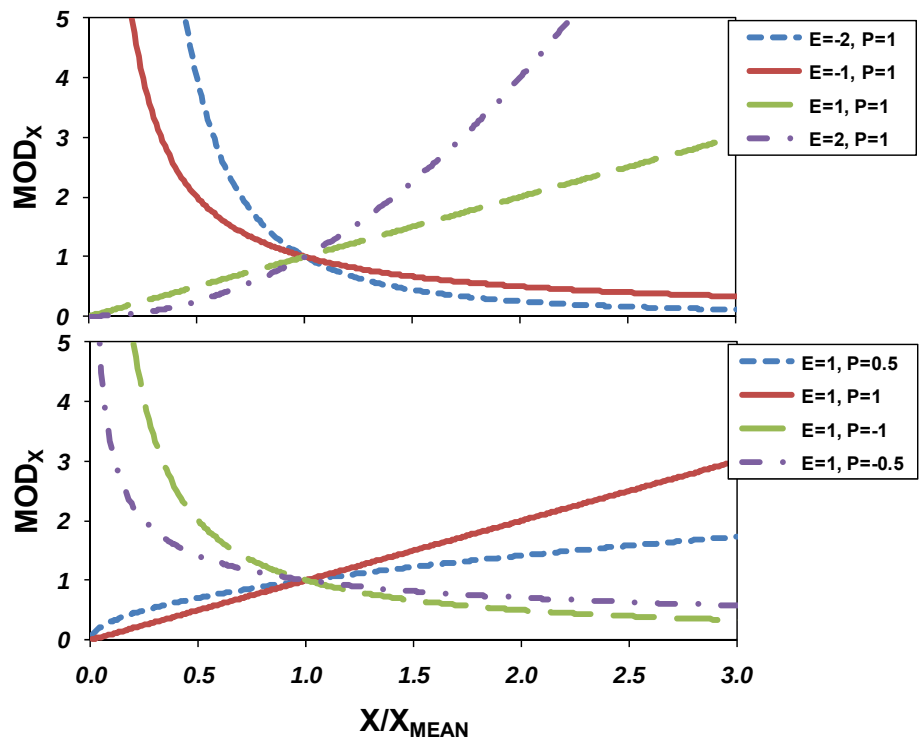

Figure 4. Examples of the functional form of modification term defined by eq. (6).

<u>Fitting Process to Account for Variables other than Copper and Fluence</u>

To achieve a better fit, multiplicative "modification terms" (eq. (6)) are introduced to eqs. (3) and (5). The form of the modification terms used, and the order in which they were introduced to the fit, were influenced by two factors: the statistical significance of the residual trends in simpler models that did not include the modification terms, and by the prior knowledge of the author regarding the findings of previous investigations concerning the effect of composition and exposure parameters on embrittlement magnitude.

A criterion was needed to determine which combination of fitting parameters constitutes a good fit to the database. When fitting models to data, a commonly used criterion is to minimize the sum of squared residuals, where a "residual" is the difference between a measurement and the model's prediction for the conditions of the measurement. However, previous efforts to fit the US-LWR surveillance database revealed that additional and/or alternative criteria are needed because the mean-square error is not very sensitive to changes in a model of the complexity needed to represent embrittlement trends in ferritic steels [Eason 98, Server 01].

The goodness-of-fit criterion used in this investigation involved minimizing the T-statistics on slopes and intercepts of lines fit to {Y = ΔT_{30} Fit Error} *vs.* {X = Regressor Variable}. Slopes and intercepts (and their standard errors) were determined by fitting the following equation:

$$\Delta T_{30(\mathrm{Pr}\,edicted)} - \Delta T_{30(Measured)} = m\Theta + b \tag{7}$$

to data for a particular regressor variable Θ (e.g. flux, fluence, copper, etc.). The *m* and *b* values in Eq. (7) were estimated using the MS-Excel® *linest* function. The T-statistic values for *m* and *b* were determined as the ratio of the estimated value of the parameter to its standard error, both of which are output by *linest*. Specifically, the T-statistics were defined as follows:

$$T_{m(\Theta)} = \frac{|m_\Theta|}{se(m)_\Theta} \qquad T_{b(\Theta)} = \frac{|b_\Theta|}{se(b)_\Theta} \tag{8}$$

Here, "se" denotes the standard error of the parenthetically indicated parameter, while the subscript indicates the regressor variable of interest.

To assess goodness-of-fit to the database as a whole, metrics quantifying the total and maximum T values (T_{TOTAL} and T_{MAX}, respectively) were calculated for each fit performed, as follows:

$$T_{TOTAL} = \sum_i T_{m(i)} + \sum_i T_{b(i)} \qquad T_{MAX} = \underset{i}{MAX}\left\{T_{m(i)}, T_{b(i)}\right\} \tag{9}$$

In both equations, "i" is an indicator denoting, respectively, all of the following variables: fluence, flux, temperature, copper, nickel, phosphorus, manganese, product form, and $\Delta T_{30(PREDICTED)}$. It is recognized that $\Delta T_{30(PREDICTED)}$ is not a regressor variable, but rather the predicted result. Nevertheless, inclusion of $\Delta T_{30(PREDICTED)}$ in the T_{TOTAL} and T_{MAX} metrics was found to result in a better overall balance of errors between the different regressor variables than when $\Delta T_{30(PREDICTED)}$ was omitted from the T_{TOTAL} and T_{MAX} metrics.

Our fitting approach involved minimizing T_{TOTAL} using the *solver* routine in MS-Excel®. The *solver* "target" was set to T_{TOTAL}, "minimize" was selected, and "by changing" cells were assigned as the variable parameters in the fit being performed. No constraints were placed on any of the variable parameters. The starting conditions (or guesses) for the variable parameters of the models that were submitted to *solver* were established by trying various parameters, or combinations of parameters, and observing which parameters or parameter combinations led to the least statistically significant residual trends. Once an acceptable combination of parameters was established through this manual process, the parameter guesses were submitted to *solver* to further improve the statistical goodness of fit.

After running *solver* to minimize T_{TOTAL}, each candidate fit was classified as follows based on the value of T_{MAX}:

<u>Unacceptable</u>: $T_{MAX} > 1.97$. This indicates a statistically significant residual trend, at the 5% significance level, for at least one of the candidate regressor variables.

<u>Provisional</u>: $1.97 > T_{MAX} > 1$. These models have no statistically significant residual trends at the 5% significance level. However, $T_{m(\Theta)}$ and $T_{b(\Theta)}$ values can be close to 1.97 in these models, and slightly different initial guesses for the parameters can lead to unacceptable models. Also, these models tend to exhibit an uneven distribution of errors among the regressor variables. For example, a provisional model may have $T_{m(Cu)}$ and $T_{b(Cu)}$ both above 1.9, while all other $T_{m(\Theta)}$ and $T_{b(\Theta)}$ values are below 0.4. The instability of provisional fits (i.e., the ease with which they could be made "unacceptable") and the heterogeneity of their error distribution among their regressor variables motivated further refinement.

<u>Acceptable</u>: $T_{MAX} < 1$. These models exhibit a reasonably homogeneous distribution of error across the regressor variables. They also are sufficiently robust so that variations in parameter guesses cannot spawn "unacceptable" models.

The fitting process continued until it identified an acceptable model, or models, after which the predictions of this model / these models were compared with ΔT_{30} data not used in the fitting process to test the predictive accuracy of these models.

FIT DEVELOPMENT

Figure 5 illustrates how the ETC fit evolved from the simple Cu/Φ model described by eqs. (2-5). Different approaches, or "tracks," were taken to model the effects of various secondary variables to determine if a similar solution was reached regardless of the track taken. The distinction between the tracks is related to different combinations of the following fitting considerations:

- <u>Order of secondary variable introduction</u>: On some tracks (1A, 1B, 2A, 2B) the secondary variables are introduced to the fit one at a time, while on other tracks (4, 5) the secondary variables are introduced to the fit all at once. When secondary variables are introduced one at a time they are allowed to influence both the M and B terms of the equation, and the order of their introduction was dictated by the magnitude of their statistical effect on the preceding fit in the series (the most significant effects being introduced first).
- <u>Treatment of Cu_{MIN} and Cu_{MAX}</u>: These variables, whose initial values of 0.07 and 0.3 (respectively), were selected based on visual inspection of the data. They exert considerable influence on the overall form of the

fit and, in the case of Cu_{MIN}, on the apportionment of embrittlement magnitude to the copper dependent *vs*. copper independent terms. For these reasons is was thought prudent to examine the effect of optimizing Cu_{MIN} and Cu_{MAX} along with all of the other fitting parameters (Tracks 2A, 2B, 4, and 5) *vs*. holding these terms fixed for most of the fit and optimizing them only near the end of the fitting track (Tracks 1A and 1B).

- Treatment of the T-statistics on the categorical variable "product form": Because the product form coefficients multiply the entirety of the M and B terms, they too exert considerable influence on the overall fit. Since the designations of "weld," "plate," and "forging" are only qualitative variables it was thought prudent to introduce them near the end of the fitting tracks only after statistically significant quantitative variables had been accounted for. However, the T-statistics on these product form terms, which are defined as follows

$$T_{PF} = \frac{1}{se(r_i)/\sqrt{n_{PF}}} \cdot \left|\sum_{i=1}^{n_{PF}} r_i\right| \qquad (10)$$

were invariably statistically significant owing to the high number or datum for each product form (in this database n_{PF} is 1067, 983, and 505 for welds, plates, and forgings, respectively). Two different approaches were taken to investigate if the resultant high T values unduly biased the fit toward placing excessive weight on a qualitative variable.

- Full weight to product form: In this approach the T statistics for the product form variables were defined according to eq. (10). This approach was followed on Tracks 1B, 2B, 4, and 5.
- Reduced weight to product form: In this approach the radical in the denominator of eq. (10) was arbitrarily set to unity early in the fit while the quantitative variables were being introduced. When the qualitative product form variable was introduced near the end of the fitting process the radical term was evaluated as it appears in eq. (10). This approach was followed on Tracks 1A and 1B.

Figure 5 illustrates how different combinations of these fitting considerations produced a sequence of models that account for different combinations of embrittlement variables, and how the goodness of fit (as measured by the global fit statistics T_{TOTAL}, T_{MAX}, and MSE) evolved as a result. At the end of the model building phase ten models had been produced that fit the data well; these each included terms for fluence, flux, temperature, Cu, Ni, P, Mn, and product form. It should be noted that along tracks where the variables were introduced one at a time there was no statistical motivation to introduce a flux term to the equation, but it was added nevertheless with a view to completeness.

Figure 6 illustrates the fit coefficients from each of the ten "full" models established at the end of the model building phase (these are the black "X" symbols on the plots). A single acceptable model was not converged to, but rather ***a range of*** acceptable models exists because there are systematic relationships between the various fit coefficients, as illustrated in Figure 7. These relationships arise as a natural consequence of the complexity of the underlying embrittlement process, the simplicity of the algebraic fitting models used here, and of the scatter in the database that makes it difficult to resolve data trends precisely.

In the model simplification phase, also illustrated by Figure 5, the fit parameters from each of the ten "full" models were averaged to provide a starting seed, model WR-C(0), which was optimized using the *solver* routine to produce model WR-C(1). In Model WR-C(1) it was noticed that both the $E_{Mn(M)}$ and $E_{P(M)}$ coefficients were very close to zero (an E or P exponent that is equal to zero has no effect on the predicted ΔT_{30} value). $E_{Mn(M)}$ and $E_{P(M)}$ were therefore set to zero in Model WR-C(2) and the quality of the fit, as judged by the T_{MAX} statistic, remained acceptable. Model WR-C(2) was then optimized using the *solver* routine to produce model WR-C(3), which was also acceptable. In Model WR-C(3) it was noticed that both the $E_{\phi(M)}$ and $E_{\phi(M)}$ coefficients were very close to zero, again suggesting that they have close to no effect on the predicted ΔT_{30} value. These coefficients were therefore set to zero in Model WR-C(4); in this case the quality of the fit, as judged by the T_{MAX} statistic, became provisional. However, when Model WR-C(4) was optimized using the *solver* routine to produce model WR-C(5) this latter model was again acceptable based on T_{MAX}. Further trials involving setting E and P coefficients to zero (no effect), or setting product form coefficients to unity (no effect) in Model WR-C(5) revealed that all of the remaining terms were needed to retain an "acceptable" fit. Model WR-C(5) was thereby established as the model recommended in the next section.

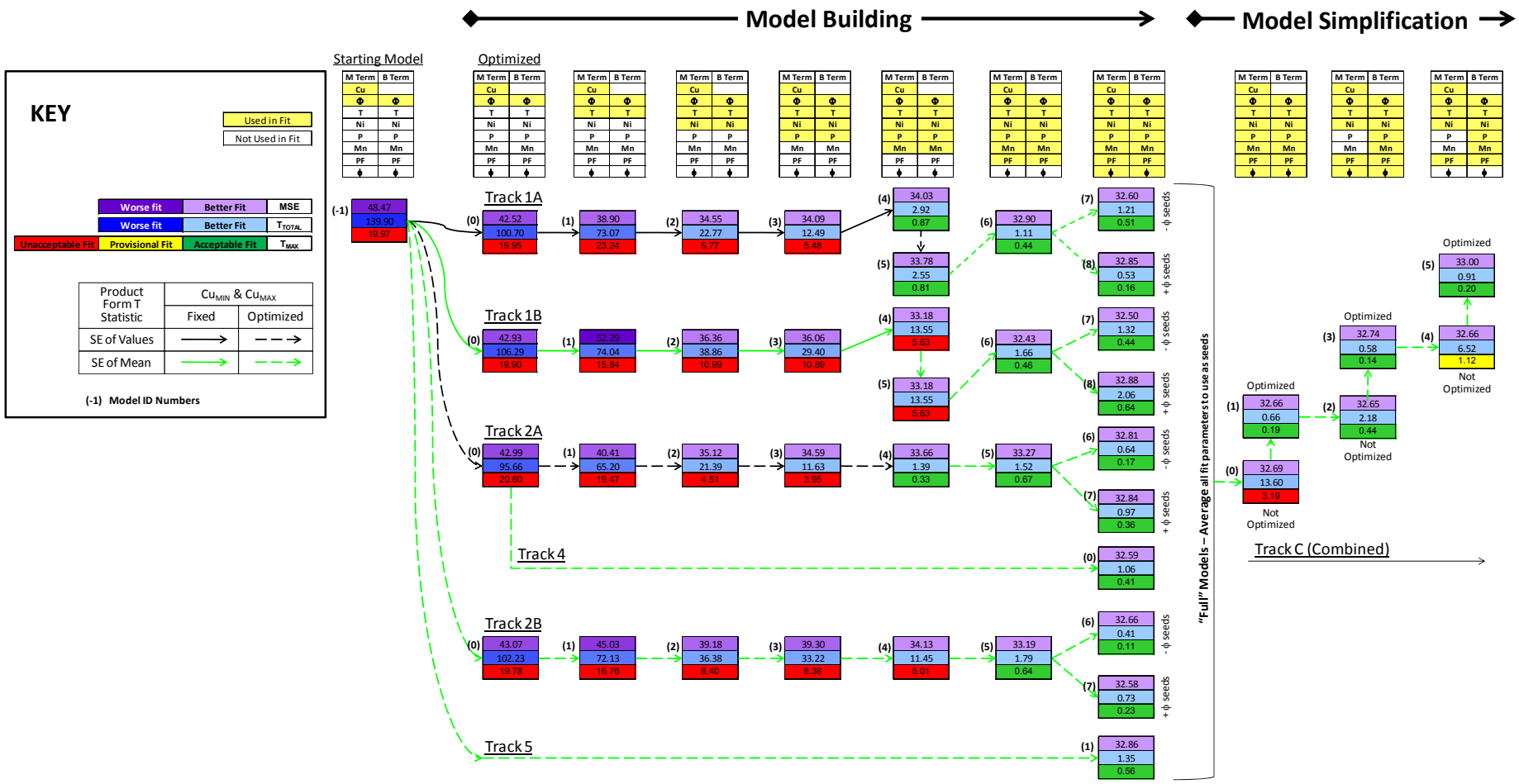

Figure 5. Diagram illustrating the development of fit WR-C(5).

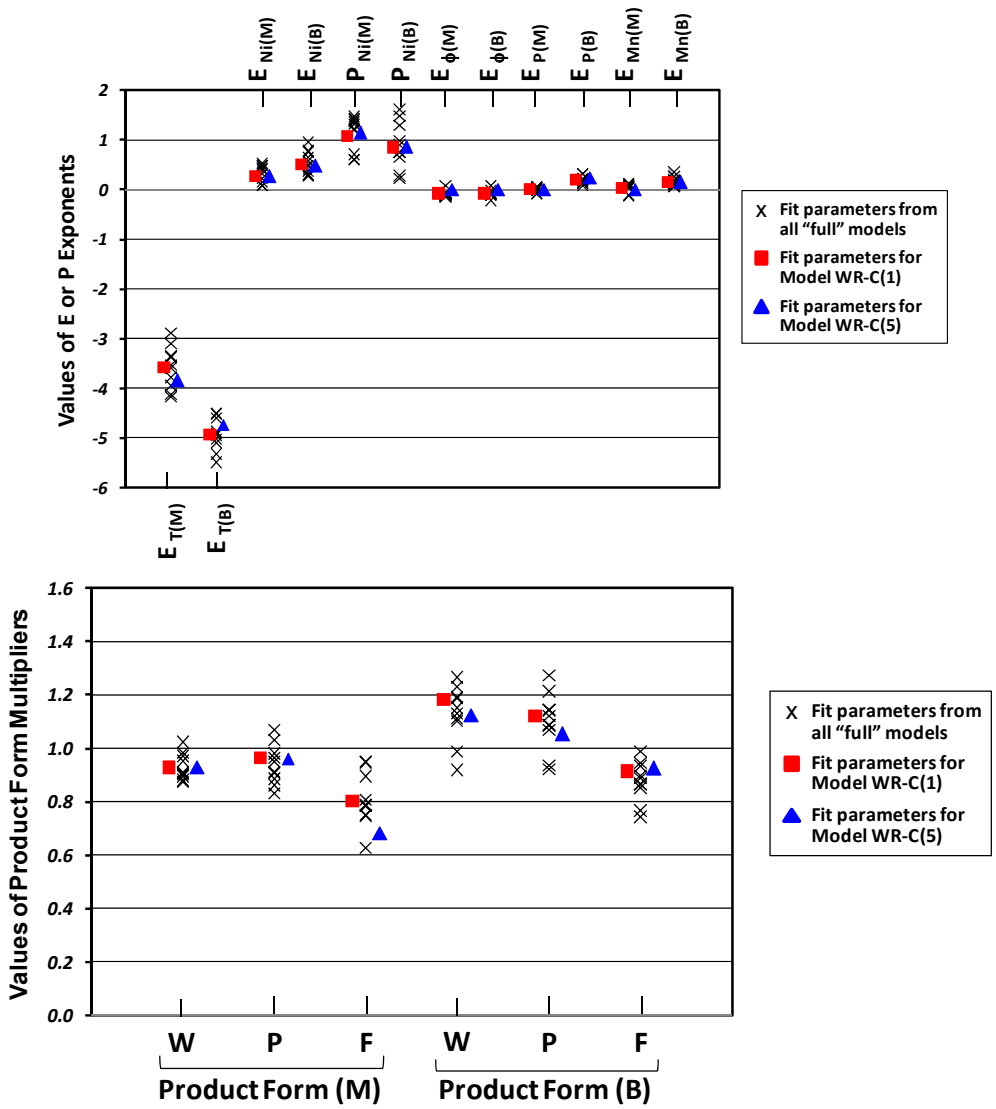

Figure 6. Fit coefficients from various models reflecting the effects of the secondary variables: quantitative (top) and qualitative (bottom).

RECOMMENDED MODEL

The fit resulting at the end of the model simplification process, denoted WR-C(5), is as follows:

$$\Delta T_{30} = MAX\begin{Bmatrix} MIN(Cu, 0.35) - 0.05 \\ - \\ 0 \end{Bmatrix} \times M + B \tag{11}$$

$$M = \begin{bmatrix} M_W = 0.93 \\ M_P = 0.96 \\ M_F = 0.68 \end{bmatrix} MAX\langle MIN\{[ln(\Phi) - ln(1.67 \times 10^{17})] \cdot 171.3, 733.5\}, 0\rangle \cdot \left[\frac{T}{550}\right]^{E_{T(M)} - 3.84} \cdot \left[\frac{(Ni)^{1.155}}{0.63}\right]^{0.28}$$

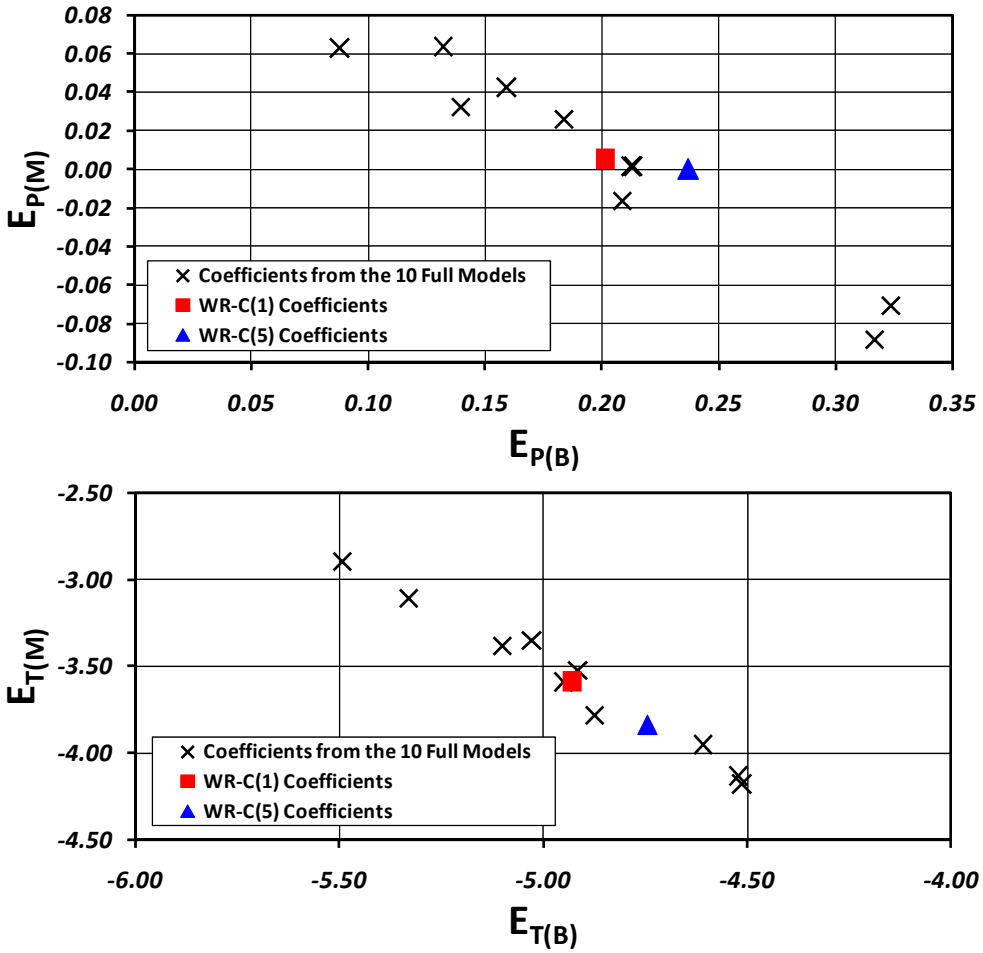

Figure 7. Illustration of some of the systematic relationships that exist between the various fit coefficients.

$$B = \begin{bmatrix} B_W = 1.12 \\ B_P = 1.056 \\ B_F = 0.925 \end{bmatrix} \cdot \{9.78 \times 10^{-10} \cdot \Phi^{0.5564}\} \cdot \left[\frac{T}{550}\right]^{-4.74} \cdot \left[\frac{P}{0.012}\right]^{0.24} \cdot \left[\frac{(Ni)^{0.865}}{0.63}\right]^{0.48} \cdot \left[\frac{Mn}{1.36}\right]^{0.15}$$

In eq. (11) the result of the formula is expressed in °F, this can be converted to °C by multiplying by $\frac{5}{9}$. Fit WR-C(5) has no statistically significant residual trends *vs*. variables that have been identified as causal, or potentially causal, in neutron irradiation embrittlement. As illustrated in Figure 8, the standard deviation for this fit increases with neutron fluence, as follows

$$\sigma = 0.073\Phi^{0.138} \tag{12}$$

ASSESSMENT OF THE WR-C(5) RELATIVE TO DATA FROM NON-TRADIATION SOURCES

As stated earlier, to develop the WR-C(5) fit we used data originating from sources not traditionally used by the NRC to develop ETCs for regulatory used. In this section we perform further assessments of prediction residuals to determine how well WR-C(5) represents embrittlement trends in both traditional and non-traditional data subsets, and to determine if inclusion of non-traditional data has skewed or biased the WR-C(5) fit relative to its ability to predict USLWR surveillance data, or the data in any other subset.

The database of 2,561 shift values partitions into five mutually exclusive and collectively exhaustive subsets:

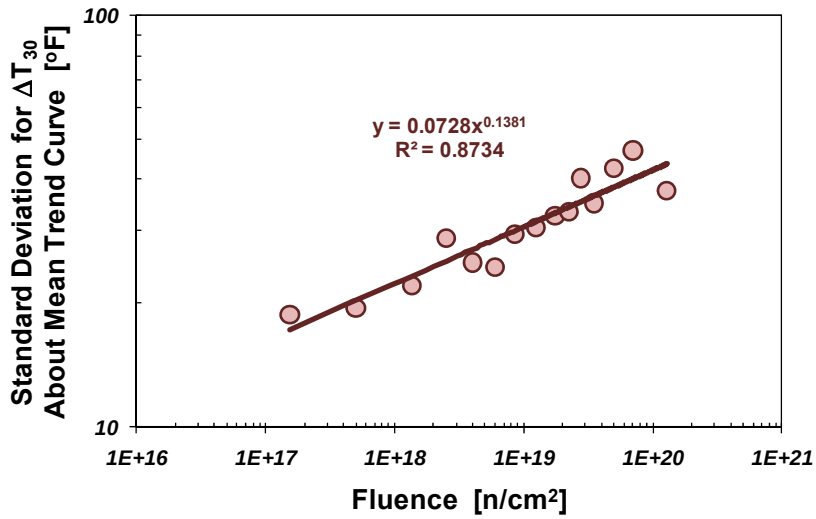

Figure 8. Effect of fluence on the standard deviation of fit WR-C(5).

- Data from traditional sources
  - o ΔT_{30} data from the USLWR Appendix H surveillance program — 936 values
- Data from non-traditional sources
  - o ΔT_{30} data from non-US surveillance programs — 248 values
  - o ΔYS data from non-US surveillance programs — 24 values
  - o ΔT_{30} data from test reactor irradiations — 573 values
  - o ΔYS data from test reactor irradiations — 780 values

The subset of 24 ΔYS shift values from non-US surveillance programs is too small to permit reliable assessment and so will not be considered further. In the following sub-sections the mean trends and scatter shown by the other four data subsets is assessed relative to the mean trends and scatter reflected by the overall fit WR-C(5).

Mean Trends

In Figure 9 through Figure 12 an assessment is made of how well the mean embrittlement trends, as expressed by WR-C(5), represent the embrittlement trends in four data subsets. The assessment is performed by examining graphs of prediction residuals plotted *vs*. two exposure variables (fluence and flux) and *vs*. two composition variables (copper and nickel). These regressor variables were selected for examination because, in the case of fluence, copper, and nickel, they are the most dominant determiners of irradiation embrittlement sensitivity. The effect of flux is also examined because of questions regarding the appropriateness of using data from both power and test reactor irradiations to inform the same ETC. If test and power reactor data follow different embrittlement trends this should be made clear by examining the residual trends shown by data subsets comprised exclusively of test and power reactor data.

The following paragraphs provide commentary on, and summarize the information in, these figures:

- ΔT_{30} data from the USLWR Appendix H surveillance program : Figure 9 assesses how well the overall fit WR-C(5) represents the traditional data subset (i.e. ΔT_{30} data from the USLWR Appendix H surveillance program, which are shown in these figures by the brightly colored points). These comparisons demonstrate that the WR-C(5) fit well represents the embrittlement trends in the traditional data subset. This suggests that while the non-traditional data (shown as grey points on these figures) extend the calibrated range of WR-C(5), they have not degraded the ability of WR-C(5) to predict ΔT_{30} data from the USLWR Appendix H surveillance program.
- ΔT_{30} data from non-US surveillance programs: Figure 10 assesses how well the overall fit WR-C(5) represents ΔT_{30} data from non-US surveillance programs, which are shown in these figures by the brightly colored points. Relative to the USLWR data, this data subset generally exists in a range of both (a) low copper, and (b) higher fluence. The embrittlement trends in this data subset are reasonably well represented

by WR-C(5) for copper, nickel, and flux. For fluence, the embrittlement trends in this data subset are reasonably well represented by WR-C(5) up to a fluence of about 3.5×10^{19} n/cm^2; above this fluence the limited data show a slight tendency toward under-prediction of embrittlement magnitude by WR-C(5). With this caveat, these data suggest that WR-C(5) provides a reasonable representation of embrittlement trends for this data subset.

- ΔT_{30} data from test reactor irradiations: Figure 11 assesses how well the overall fit WR-C(5) represents ΔT_{30} data from test reactor irradiations, which are shown in these figures by the brightly colored points. Relative to the USLWR data, this data subset covers a similar range of copper and nickel but, of course, concentrates in the high flux and/or high fluence régimes. The embrittlement trends in this data subset are reasonably well represented by WR-C(5) for copper, fluence, and flux. The observation that WR-C(5) provides as reasonable a representation of the flux and fluence trends in this ***test reactor*** data subset as it did in the two ***power reactor*** data subsets despite the fact that WR-C(5) includes no terms that account for flux is important, for it indicates that there is no compelling empirical reason to treat test and power reactor data separately.

  This data subset includes the highest nickel data in the entire database. At nickel contents typical to the rest of the database, i.e., below about 1.2 weight percent, the overall trends expressed by WR-C(5) match those in this data subset reasonably well. However for the very high nickel contents (1.5 weight percent and above) this data subset reveals that WR-C(5) significantly under-predicts the embrittlement magnitude.
- ΔYS data from test reactor irradiations: Figure 12 and assesses how well the overall fit WR-C(5) represents ΔYS data from test reactor irradiations, which are shown in these figures by the brightly colored points. Relative to the USLWR data, this data subset covers a similar range of copper and nickel but, of course, concentrates in the high flux and/or high fluence régimes. The embrittlement trends in this data subset are reasonably well represented by WR-C(5) for copper, nickel, fluence, and flux. The observation that WR-C(5) provides as reasonable a representation of the flux and fluence trends in this ***test reactor*** data subset as it did in the two ***power reactor*** data subsets despite the fact that WR-C(5) includes no terms that account for flux is important, for it indicates that there is no compelling empirical reason to treat test and power reactor data separately.

In summary, the comparisons made in Figure 9 through Figure 12 demonstrate that WR-C(5), which was fit to the entire database, also represents the embrittlement trends in both traditional and non-traditional data subsets with reasonable accuracy. Specifically, no major differences in embrittlement trends are seen between the traditional data subset (i.e. ΔT_{30} data from US power reactor surveillance programs) and three non-traditional data subsets (i.e., ΔT_{30} data from non-US surveillance programs, ΔT_{30} data from test reactor irradiations, and ΔYS data from test reactor irradiations). These findings demonstrate that a single ETC is capable of representing embrittlement trends, as quantified by ΔT_{30} and ΔYS in both power and test reactor data, and in both US and non-US surveillance data, with equivalent accuracy. It is important to note that these statements cannot be made regarding ETCs in current regulatory use, which fail to capture embrittlement trends at fluences above approximately $2\text{-}3 \times 10^{19}$ n/cm^2 [EricksonKirk 08a, EricksonKirk 08b].

Scatter about the Mean

Figure 13 compares the scatter about the mean prediction, and its increase with fluence, as represented by eq. (11) for the whole database to which WR-C(5) was fit (black line and black/red plotting symbol) with the scatter about the mean prediction, and its increase with fluence, for the four data subsets examined previously. The (x,y) coordinates of the plotting symbols in this figure were determined as follows:

- A data set, or subset, was identified
- A fluence range was identified.
- The x coordinate in Figure 13 was defined as the mean fluence of all observations within the fluence range for the data subset of interest.
- The y coordinate in Figure 13 was defined as the standard deviation of all WR-C(5) prediction residuals within the fluence range for the data subset of interest.

The data in Figure 13 support the following conclusions:

a) The observation that the scatter about the mean prediction increases with increasing fluence, while it has not to the author's knowledge been noted before, is not an artifact of the combined database, nor of any data subset. This trend is manifest throughout the available data and, indeed, can be seen within the traditional ΔT_{30} data from USLWR power reactor surveillance programs.
b) Of the data subsets examined all show somewhat less scatter than is reflected by the trend for the database as a whole, except for the subset of ΔT_{30} shift values from test reactor irradiations, which show

.

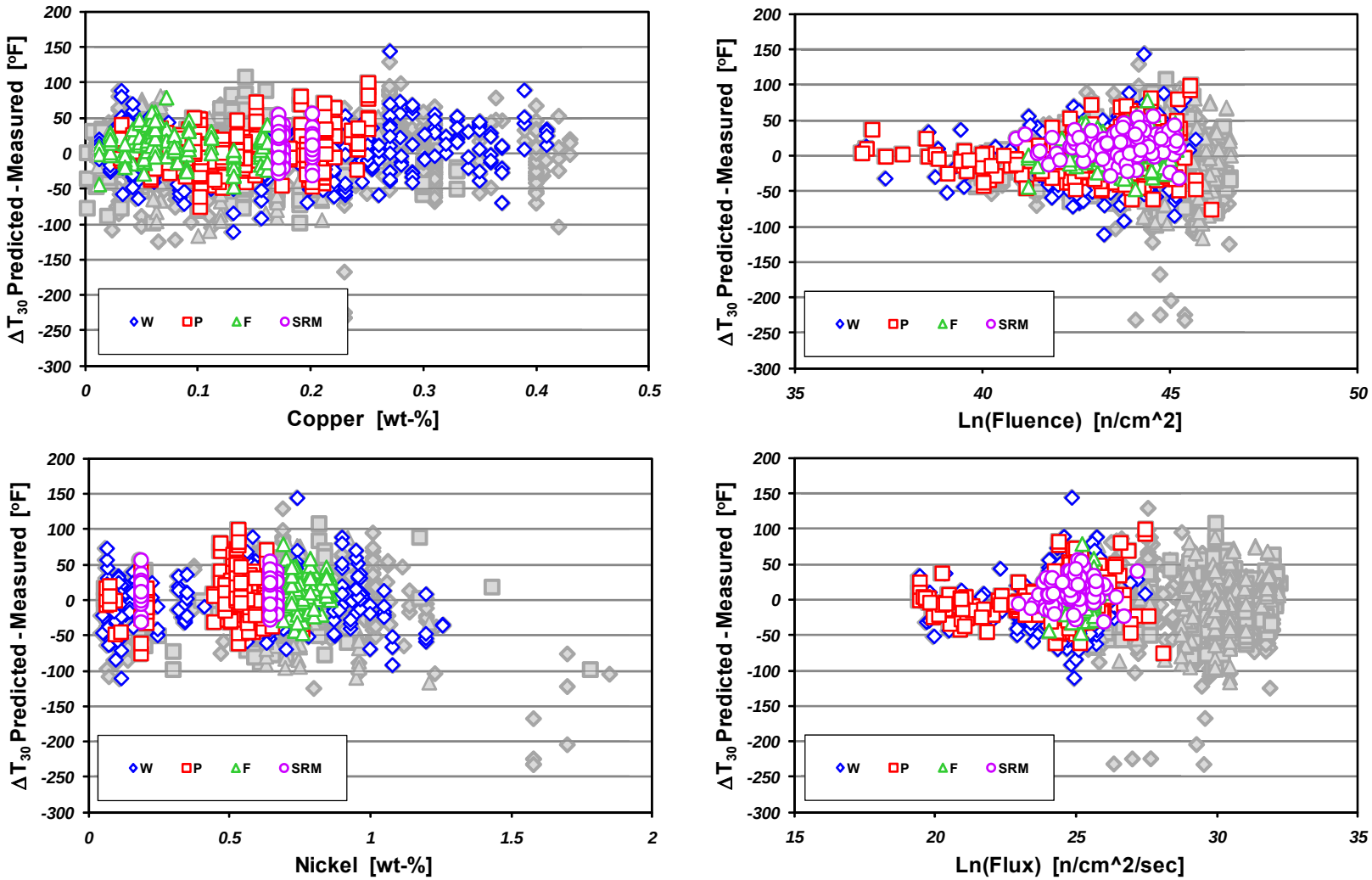

Figure 9. WR-C(5) prediction residuals for the USLWR power reactor ΔT_{30} data (colored points) compared to entire database (grey points).

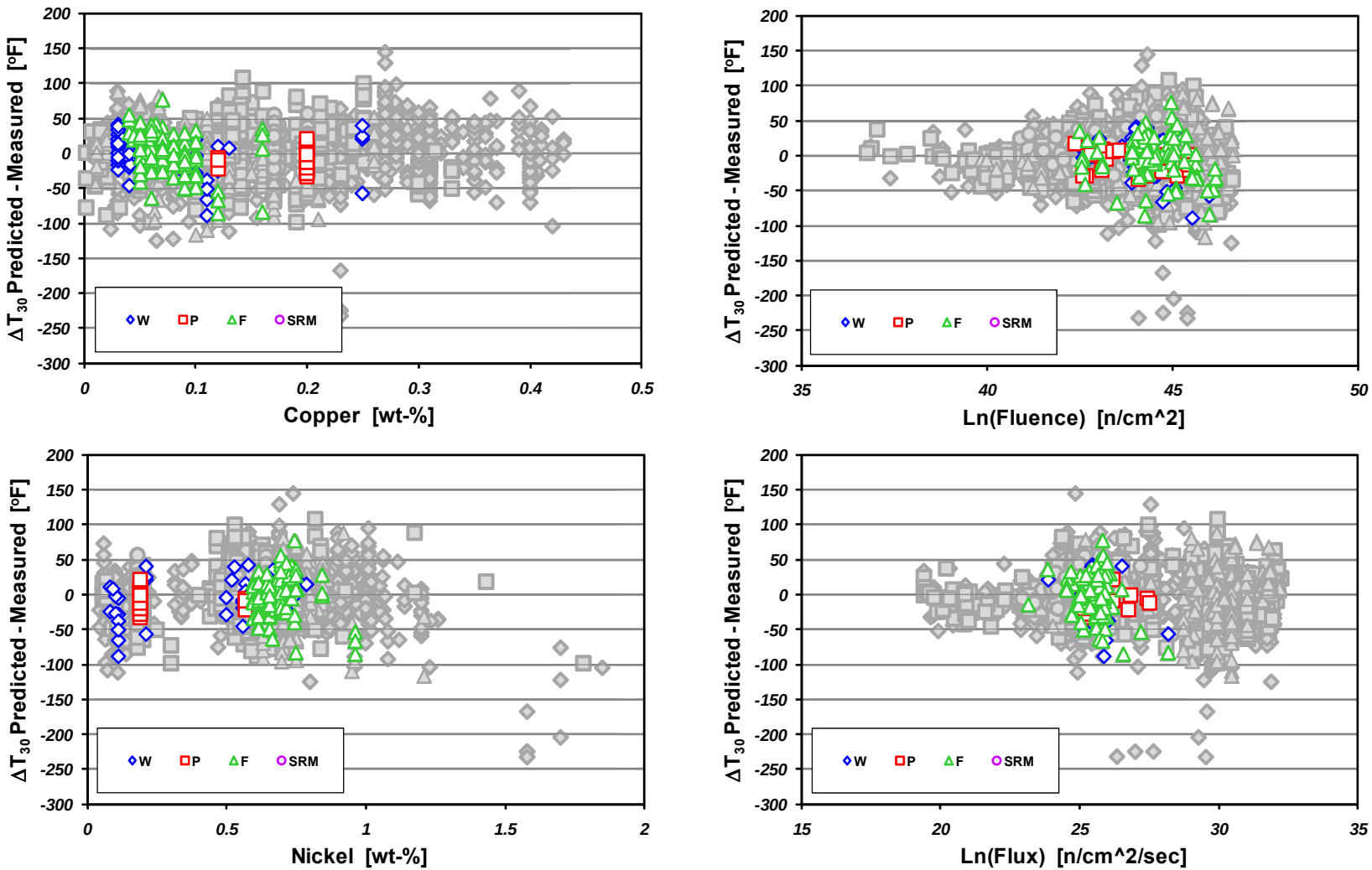

Figure 10. WR-C(5) prediction residuals for non-US power reactor ΔT_{30} data (colored points) compared to entire database (grey points).

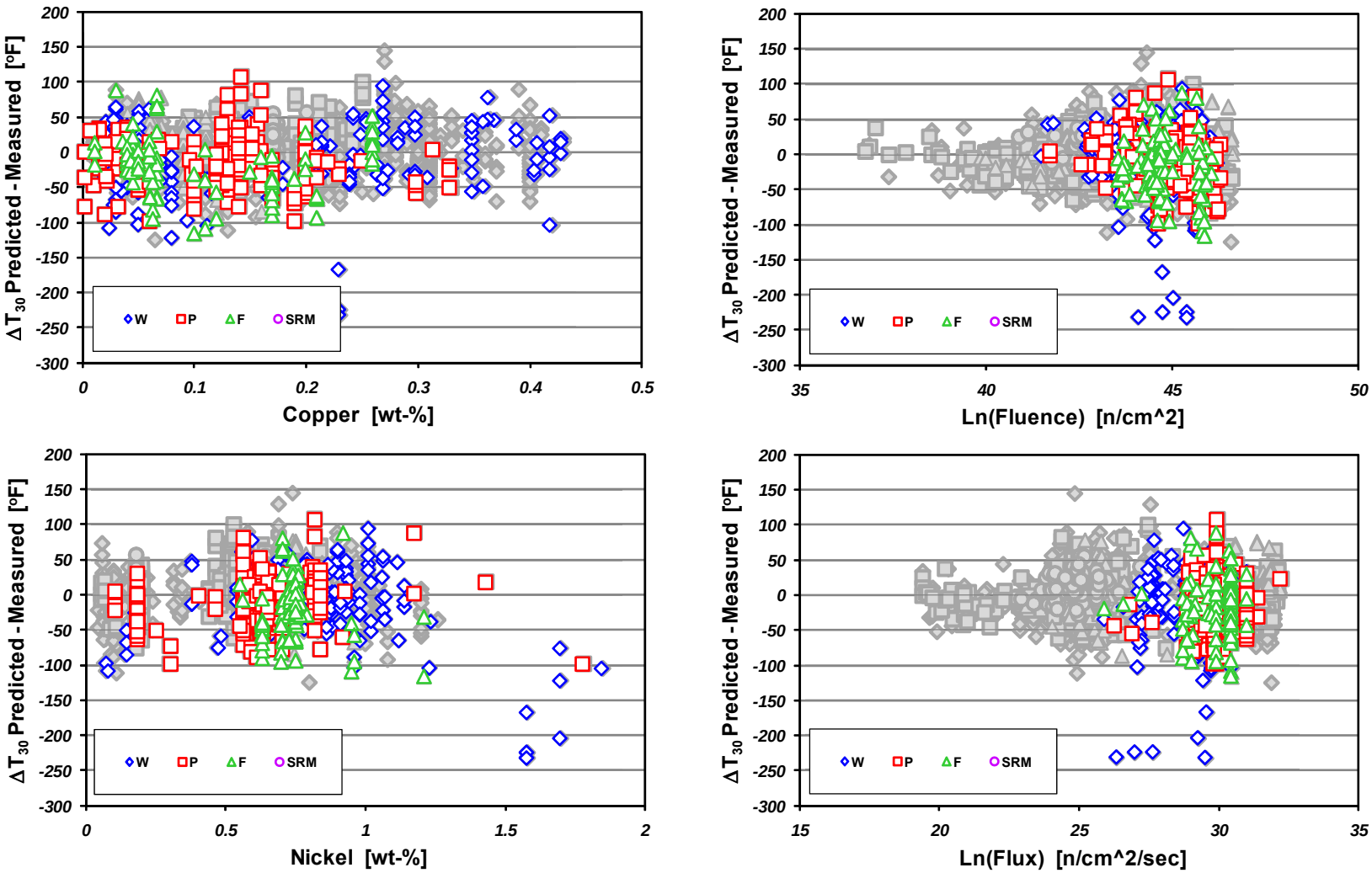

Figure 11. WR-C(5) prediction residuals for test reactor ΔT_{30} data (colored points) compared to entire database (grey points).

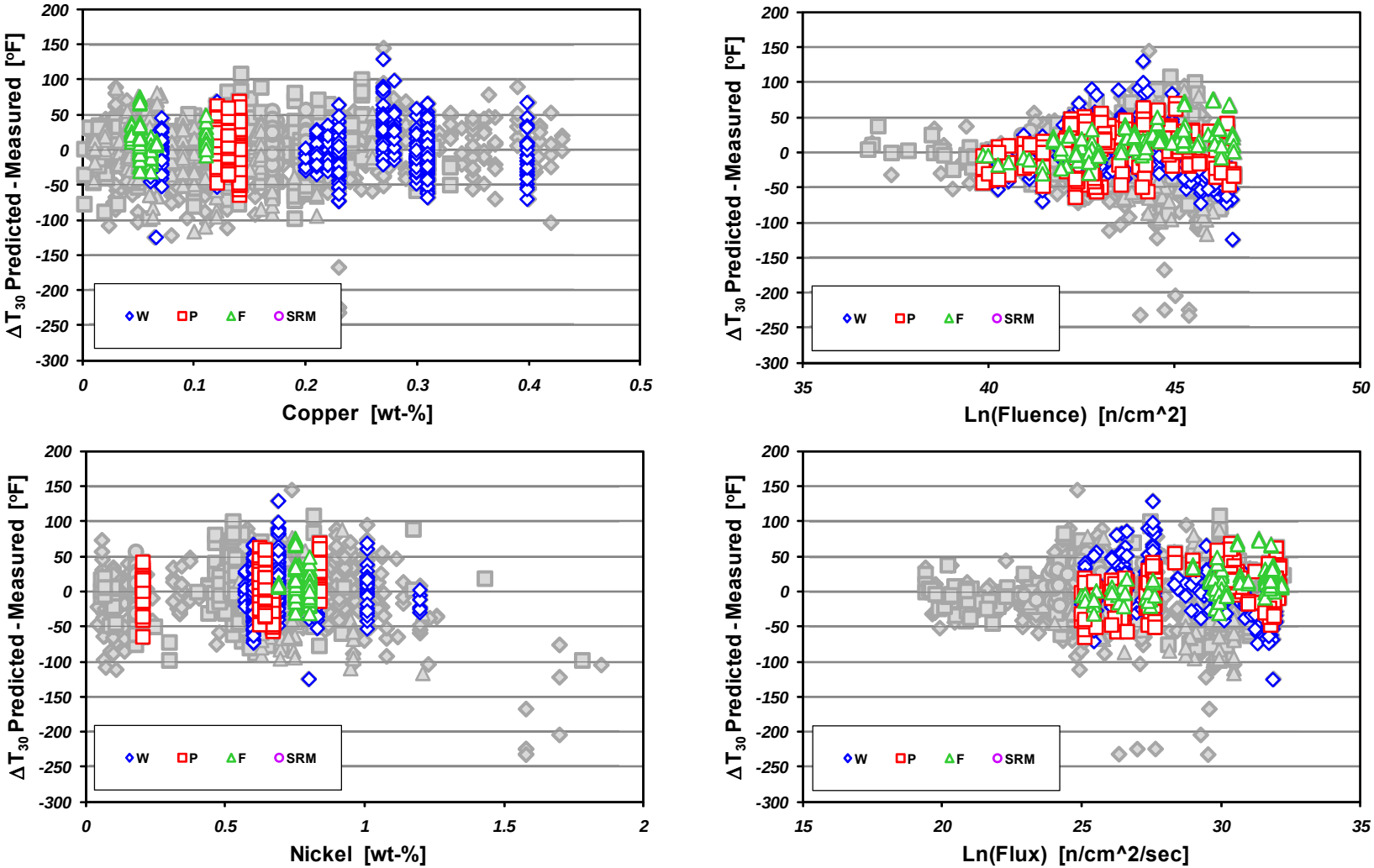

Figure 12. WR-C(5) prediction residuals for test reactor ΔYS data (colored points) compared to entire database (grey points).

more scatter than is characteristic of the database as a whole. This may occur because this data subset represents among the oldest data in the database, and was assembled from the widest diversity of investigators.

c) The scatter trend with increasing fluence for the traditional ΔT_{30} data from USLWR power reactor surveillance programs is, if anything, slightly overestimated by the scatter trend for the WR-C(5) fit, which is that for the whole database. In applications, this overestimation of scatter can be regarded as an implicit conservatism.

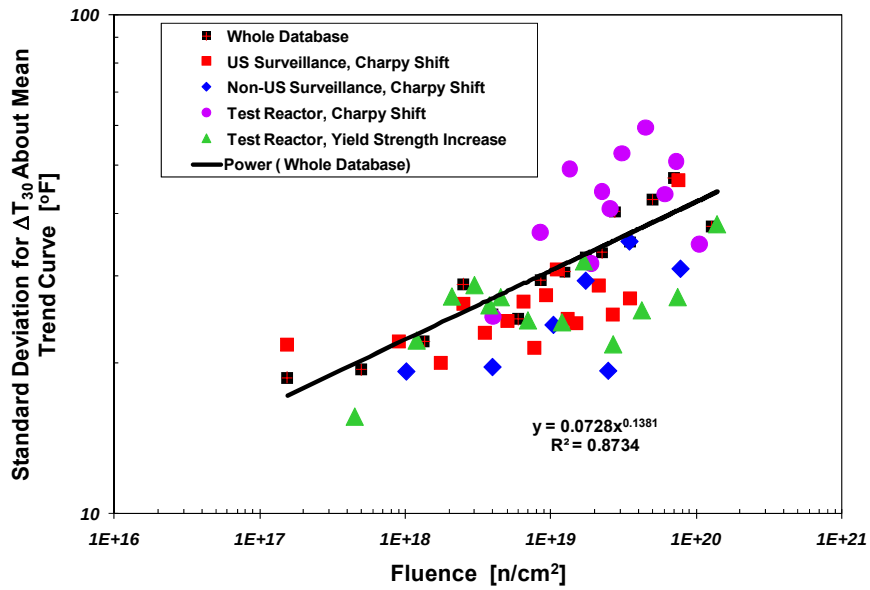

Figure 13. Scatter about the mean embrittlement trend, and its increase with increasing fluence, expressed by the WR-C(5) model (solid line) compared to that of different data subsets.

SUMMARY

In this study we have used a wide range of data quantifying the changes produced on the mechanical properties of nuclear RPV steels by neutron irradiation embrittlement to develop an empirically fit trend curve. This curve represents the effect of chemical composition and exposure parameters on the shift in the Charpy V-notch energy transition temperature. The data used to develop the fit comes from a wider variety of sources (i.e., both power reactors and test reactors, both US and non-US power reactor surveillance) than has been used as the basis for fitting such trend curves in the United States. Nevertheless, comparisons presented herein indicate that a single algebraic model, denoted WR-C(5), represents reasonably well both the trends evident in the data overall as well as trends exhibited by the following four data subsets:

- ΔT_{30} data from the US surveillance program
- ΔT_{30} data from non-US surveillance programs
- ΔT_{30} data from test reactor irradiations
- ΔYS data from test reactor irradiations

Of particular importance, the WR-C(5) model indicates the existence of trends in high fluence data ($\Phi > 2\text{-}3\times10^{19}$ n/cm^2, E > 1MeV) that are not as apparent in the US surveillance data due to the limited quantity of ΔT_{30} data measured at high fluence in this dataset. Additionally, WR-C(5) models well the trends in both test and power reactor data despite the fact it has not term to account for flux. While the appropriateness of using data from such a variety of sources to inform a trend curve is debated by the technical community, it is suggested that one appropriate use of the WR-C(5) trend curve may include the design irradiation studies to validate or refute the findings presented herein. Additionally, WR-C(5) could be used, along with other information (e.g., other trend curves, theoretical expectations, plant-specific data, etc.), as one tool to predict irradiation trends pending the availability of confirmatory data in the high fluence régime

REFERENCES

10CFR5061a — Title 10, Section 50.61a, of the *Code of Federal Regulations*, "Alternative Fracture Toughness Requirements for Protection against Pressurized Thermal Shock Events," promulgated January 4, 2010.

Brillaud 92 — Brillaud, C., and Hedin, F., "In-Service Evaluation of French Pressurized-Water Reactor Vessel Steel," *Effects of Radiation on Materials, 15th International Symposium,* ASTM STP-1125, R.E. Stoller, A.S. Kumar, and D.S. Gelles, Eds., American Society for Testing and Materials, 1992, pp. 23–49.

Brillaud 01 — Brillaud, C., Grandjean, Y., and Saillet, S., "Vessel Investigation Program of 'CHOOZ A' PWR Reactor after Shutdown," *Effects of Radiation on Materials: 20th International Symposium, ASTM STP 1405*, S.T. Rosinski, M.L. Grossbeck, T.R. Allen, and A.S. Kumar, Eds., American Society for Testing and Materials, West Conshohocken Pennsylvania, 2001, pp. 28-41.

Bellman 90 — Bellmann, D., and Ahlf, J., "Comparison of Experimental 41J Shifts with the Predictions of German KTA 3203 and U.S. NRC Regulatory Guide 1.99," *Effects of Radiation on Materials: 14th International Symposium, ASTM STP 1046*, N.H. Packin, R.E. Stoller, and A.S. Kumar, Eds., American Society for Testing and Materials, Philadelphia, 1990, pp. 265-283.

Chaouadi 05a — R. Chaouadi, "An Engineering Radiation Hardening Model for RPV Materials," SCK/CEN Report R-4235, September 2005.

Chaouadi 05b — R. Chaouadi, and R. Gérard, "Copper Precipitate Hardening of Irradiated RPV Materials and Implications on the Superposition Law and Re-Irradiation Kinetics," *Journal of Nuclear Materials,* **345** (2005), pp. 65–74.

Eason 98 — Eason, E.D., J.E. Wright, and G.R. Odette, "Improved Embrittlement Correlations for Reactor Pressure Vessel Steels," NUREG/CR-6551, U.S. Nuclear Regulatory Commission, Washington DC, 1998.

Eason 07 — Eason, E.D., Odette, G.R., Nanstad, R.K., and Yamamoto, T., "A Physically Based Correlation of Irradiation Induced Transition Temperature Shifts for RPV Steel," Oak Ridge National Laboratory, ORNL/TM-2006/530, http://www.nrc.gov/reading-rm/adams/web-based.html, ADAMS ML081000630.

EricksonKirk 08a — "Technical Basis for Revision of Regulatory Guide 1.99: NRC Guidance on Methods to Estimate the Effects of Radiation Embrittlement on the Charpy V-Notch Impact Toughness of Reactor Vessel Materials," DRAFT report, http://www.nrc.gov/reading-rm/adams/web-based.html, ADAMS ML081120289.

EricksonKIrk 08b — "Further Evaluation of High Fluence Data," http://www.nrc.gov/reading-rm/adams/web-based.html, ML081120600

Fabry 96 — Fabry, A., et al., "Research to Understand the Embrittlement Behavior of Yankee/BR3 Surveillance Plate and Other Outlier RPV Steels," *Effects of Radiation on Materials: 17th International Symposium, ASTM STP 1270*, D.S. Gelles, R.K. Nanstad, A.S. Kumar, and E.A. Little, Eds., American Society for Testing and Materials, Philadelphia, 1996, pp. 138-187.

GALL — "Generic Aging Lessons Learned (GALL) Report: Summary," NUREG-1801, U.S. Nuclear Regulatory Commission, http://www.nrc.gov/reading-rm/doc-collections/nuregs/staff/sr1801/initial .

Gérard 06 — Gérard, R., E. Lucon, M. Scibetta, R. Chaouadi, and E. Van Walle, "Reactor Pressure Vessel Steels Embrittlement at Very High Neutron Doses," *Fontevraud 6th International Symposium on Contribution of Material Investigations to Improve Safety and Performance of LWRs*, September 18–22, 2006, Fontevraud-L'Abbaye, France

Hawthorne 85 — Hawthorne, J.R., Menke, B.H., and Hiser, A.L., "Notch Ductility and Fracture Toughness Degradation of Pressure Vessel Steel Reference Plates from Pool Side Facility (PSF) Irradiation Capsules," *Effects of Radiation on Materials: 12th International Symposium,*

ASTM STP 870, F.A. Garner and J.S. Perrin, Eds., American Society for Testing and Materials, Philadelphia, 1985, pp. 1163-1186.

IAEA CRP-1 — IAEA-176, "Co-ordinated Research Programme on Irradiation Embrittlement of Pressure Vessel Steels," International Atomic Energy Agency, 1975.

IAEA CRP-2 — TRS-265, "Analysis of the Behaviour of Advanced Reactor Pressure Vessel Steels under Neutron Irradiation," 1986.

IAEA CRP-3 — Unpublished Report and Database: Optimizing of Reactor Pressure Vessel Surveillance Programmes and their Analyses

IAEA 1442 — *Guidelines for Prediction of Irradiation Embrittlement of Operating WWER-440 Reactor Pressure Vessels*, prepared within the framework of the coordinated research project, IAEA TECHDOC 1442, June 2005.

Ishino 90 — Ishino S, Kawakami T, Hidaka T, and Satoh M., "The effect of chemical composition on irradiation embrittlement," *Nucl Eng Des* 1990(119): 139–48.

JNES 07 — JNES-SS-0707, "Accuracy and Reliability of the Revised Transition Temperature Shift Prediction in the Japan Electrical Association Code.

Kirk 01 — Kirk, M., and M.E. Natishan, "Shift in Toughness Transition Temperature Due to Radiation: ΔT_o *vs.* ΔT_{41J}, A Comparison and Rationalization of Differences," *Proceedings of the IAEA Specialists Meeting on Master Curve Technology*, Prague, Czech Republic, September 2001.

Kussmaul 90 — Kussmaul, K., Föhl, J., and Weissenberg, T., "Investigation of Materials from a Decommissioned Reactor Pressure Vessel – A Contribution to the Understanding of Irradiation Embrittlement, *Effects of Radiation on Materials: 14th International Symposium, ASTM STP 1046*, N.H. Packin, R.E. Stoller, and A.S. Kumar, Eds., American Society for Testing and Materials, Philadelphia, 1990, pp. 80-104.

Lee 01 — Lee, B-S., Yang, W-J., Huh, M-Y., Chi, S-H., and Hong, J-H.,"Master Curve Characterization of Irradiation Embrittlement Using Standard and 1/3-Sized Precracked Charpy Specimens," *Effects of Radiation on Materials: 20th International Symposium, ASTM STP 1405*, S.T. Rosinski, M.L. Grossbeck, T.R. Allen, and A.S. Kumar, Eds., American Society for Testing and Materials, West Conshohocken Pennsylvania, 2001, pp. 55-67.

Leitz 93 — Leitz, C., Klausnitzer, E.N., and Hofmann, G., "Annealing Experiments on Irradiated NiCrMo Weld Metal," *Effects of Radiation on Materials: 16th International Symposium, ASTM STP 1175*, A.S. Kumar, D.S. Gelles, R.K. Nanstad, and E.A. Little, Eds., American Society for Testing and Materials, Philadelphia, 1993, pp. 352-362.

Nanstad 04 — Nanstad, R.K., et al., "Fracture Toughness, Thermo-Electric Power, and Atom Probe Investigations of JRQ Steel in I, IA, IAR, and IARA Conditions," *Effects of Radiation on Materials: 22nd International Symposium, ASTM STP 1475*, T.R. Allen, R.G. Lott, J.T. Busby, and A.S. Kumar, Eds., American Society for Testing and Materials, West Conshohocken Pennsylvania, 2006, pp. 195-211.

Onizawa 01 — Onizawa, K., and Suzuki, M., "Comparison of Transition Temperature Shifts Between Static Fracture Toughness and Charpy-v Impact Properties Due to Irradiation and Post-Irradiation Annealing for Japanese A533B-1 Steels," *Effects of Radiation on Materials: 20th International Symposium, ASTM STP 1405*, S.T. Rosinski, M.L. Grossbeck, T.R. Allen, and A.S. Kumar, Eds., American Society for Testing and Materials, West Conshohocken Pennsylvania, 2001, pp. 79-96.

Pachur 93 — Pachur, D., "Comparison of Drop-Weight and Instrumented Charpy Impact Test Results for Irradiated RPV," *Effects of Radiation on Materials: 16th International Symposium, ASTM STP 1175*, A.S. Kumar, D.S. Gelles, R.K. Nanstad, and E.A. Little, Eds., American Society for Testing and Materials, Philadelphia, 1993, pp. 195-210.

Randall 87 — Randall, P.N., "Basis for Revision 2 of the U.S. Nuclear Regulatory Commission's Regulatory Guide 1.99," *Radiation Embrittlement in Nuclear Pressure Vessel Steels: An International Review* (Second Volume), ASTM STP-909, L.E. Steele, Ed., 1987.

RG199R2 Regulatory Guide 1.99, “Radiation Embrittlement of Reactor Vessel Materials,” Rev. 2, U.S. Nuclear Regulatory Commission, Washington, DC, May 1988.

Server 01 Server, W., C. English, D. Naimon, and S. Rosinski, “Charpy Embrittlement Correlations—Status of Combined Mechanistic and Statistical Bases for U.S. RPV Steels – MRP-45,” PWR Materials Reliability Program (PWRMRP), Electric Power Research Institute, Palo Alto, California, 2001.

Stallmann 94 E W. Stallmann, J. A. Wang, E B., and K. Kam, “TR-EDB: Test Reactor Embrittlement Data Base, Version 1,” NUREG/CR-6076, United States Nuclear Regulatory Commission, 1994.

Williams 86 Williams T.J., et al., "The Influence of Copper, Nickel and Irradiation Temperature on the Irradiation Shift of Low Alloy Steels,” *Proceedings of 2nd International Symposium on Environmental Degradation of Materials in Nuclear Power Systems —Water Reactors*, September 1985, American Nuclear Society, 1986.